

Article

Non-Contact Impact Source Localization in Composite Symmetry Panels Based on A_0 Mode of Lamb Waves

Ziping Wang^{1,2,*} , Jiazhen Zhang^{1,2}, Hangrui Cui^{1,2}, Rahim Gorgin^{1,2} and Yang Zhang³

¹ Faculty of Civil Engineering and Mechanics, Jiangsu University, Zhenjiang 212013, China; 2212223013@stmail.ujs.edu.cn (J.Z.); rgorgin@ujs.edu.cn (R.G.)

² National Center for International Research on Structural Health Management of Critical Components, Jiangsu University, Zhenjiang 212013, China

³ Institute of Fluid-Flow Machinery, Polish Academy of Sciences, 80-231 Gdańsk, Poland; yzhang@imp.gda.pl

* Correspondence: wzp@ujs.edu.cn

Abstract: Traditional methods for detecting damage in engineering structures often use offline static damage detection. To enable the real-time and precise identification of dynamic damage while maintaining symmetry in engineering structures, this study primarily concentrates on isotropic plate structures widely employed in engineering. Moreover, fiberglass board composite plates were opted as a specific research object. By utilizing the weak S_0 mode signals generated by low-frequency ultrasonic Lamb waves, the non-stationary A_0 wave signals in the composite symmetry plate structure are collected using the non-contact SLDV (Scanning Laser Doppler Vibrometer) technique. The frequency characteristic parameters in the vibration signals are obtained through HHT (Hilbert–Huang Transform) analysis, followed by filtering and noise reduction. Finally, the circular trajectory intersection method is employed to accurately locate dynamic damage sources in plate structures with different material properties, thereby validating the positioning effect of contact sensors in detecting impacts caused by random impulses.

Keywords: circular trajectory intersection method; HHT (Hilbert–Huang Transform); SLDV (Scanning Laser Doppler Vibrometer); lame wave; symmetry structure localization



Citation: Wang, Z.; Zhang, J.; Cui, H.; Gorgin, R.; Zhang, Y. Non-Contact Impact Source Localization in Composite Symmetry Panels Based on A_0 Mode of Lamb Waves. *Symmetry* **2023**, *15*, 1836. <https://doi.org/10.3390/sym15101836>

Academic Editor: Sergei D. Odintsov

Received: 12 August 2023

Revised: 18 September 2023

Accepted: 25 September 2023

Published: 28 September 2023



Copyright: © 2023 by the authors. Licensee MDPI, Basel, Switzerland. This article is an open access article distributed under the terms and conditions of the Creative Commons Attribution (CC BY) license (<https://creativecommons.org/licenses/by/4.0/>).

1. Introduction

The propagation characteristics of elastic waves in isotropic homogeneous media are generally classified into two categories: wave characteristics in infinite isotropic elastic bodies and wave characteristics in finite elastic bodies, including properties such as wave reflection, refraction, scattering, and plane wave behavior within structures [1–3]. Different vibration sources, due to their different causative mechanisms, result in distinct acoustic wave characteristics [4]. Therefore, dynamic signals generated by internal cracks, lattice dislocations, fiber fractures, and other sources of damage occurring and propagating within a material exhibit different dynamic properties [5]. Consequently, when ultrasound waves propagate in different media, they are influenced by factors such as the physical properties of the medium and the presence of damage sources. In practical applications, it is necessary to consider multiple factors comprehensively to obtain accurate detection results.

Composite materials are composed of two or more materials with different physical and chemical properties, resulting in anisotropic characteristics that differ from those of single materials. The symmetry structure of composite materials is highly complex, and there are various forms of internal damage, such as delamination, debonding, matrix fracture, and others. The propagation of elastic waves in composite structures is influenced by multiple factors, especially when coupled with damage, making the wave propagation process and characteristics within the composite material more complex [6]. Consequently, the propagation characteristics of ultrasound Lamb waves, which are suitable for damage detection in isotropic homogeneous plate structures, also exhibit features such as skew

effects in composite panel structures [7,8]. Additionally, the phase velocity values of different Lamb wave modes in different directions are not the same, causing the wavefront of Lamb waves to be non-circular during propagation, as well as exhibiting anisotropic characteristics.

In the traditional damage detection of plate structures, a sensing network (contact-based) is typically applied, which is attached to the surface of the structure to primarily pick up the S_0 mode signals in Lamb waves. The S_0 mode waves in the plate structure remain relatively stable in the low-frequency range, making it easier to mitigate the effects of frequency dispersion. However, when using non-contact sensing methods to capture relevant information on the structural damage, the collected Lamb wave signals primarily consist of the A_0 mode. The A_0 mode of Lamb waves exhibits nonlinear, non-stationary frequency dispersion, and multimodal characteristics [9,10]. This can lead to inaccuracies in determining the transit time on which the localization of damage relies, ultimately affecting the precise positioning of the damage source.

The approach and preferred method for dealing with nonlinear and non-stationary ultrasonic-guided wave signals involve a linearization of the system [11]. Ultrasonic-guided wave signals are generally considered stationary or piecewise stationary, and appropriate analysis methods such as short-time Fourier transform [12], wavelet transform [13], etc., can be used to obtain the time-frequency distribution information of the signals. Among various analysis methods for ultrasonic signals, the time-domain analysis refers to analyzing the complete information of the signal in the time domain. It commonly involves parameters that describe the temporal characteristics of the waveform, such as the maximum amplitude and autocorrelation function [14,15]. However, the time-domain analysis cannot fully reflect the local features of the damage-related signals and can only provide overall information contained in the signal. Its ability to identify local signal features is limited, making it challenging to detect defect damage through a time-domain analysis. Spectral analysis, based on Fourier transform, calculates the amplitude components, power, and phase of different frequency components in the signal, allowing the spectrum to reflect the time-frequency position of the signal's spectral peaks and their temporal variations [16]. However, it is only suitable for analyzing stationary signals and cannot fully capture the essential characteristics of non-stationary signals at a particular moment [17]. Time-frequency domain analysis, on the other hand, is an analysis method that combines both time and frequency. It can analyze non-stationary signals and provide a more comprehensive description of the signal's characteristics and energy distribution in different time and frequency domains. It captures the relationship between local frequency and time, making it suitable for a comprehensive analysis and damage-related analysis of signals in the time-frequency domain [18]. In practice, ultrasonic waveforms contain comprehensive damage signal information. In recent years, the waveform analysis has shown high recognition and analysis capabilities for signals, enabling the acquisition of comprehensive damage information. Extracting relevant damage feature information using waveform analysis methods can effectively assess damage.

The combination of the well-known Hilbert spectral analysis (HAS) and the recently developed empirical mode decomposition (EMD), designated as the Hilbert–Huang transform (HHT) by NASA, indeed, represents a paradigm shift of data analysis methodology [19]. HHT is specially designed for analyzing nonlinear and non-stationary data. The key part of HHT is EMD, which can be used to decompose any complex data set into a finite and usually a small number of intrinsic modulus functions (IMF). Using the instantaneous frequency defined by the Hilbert transform to represent the physical meaning of local phase changes is better for IMF than for any other non-IMF time series. This decomposition method is adaptive and thus efficient. Since the decomposition is based on the local properties of the data, it is suitable for nonlinear and non-stationary processes [20].

Based on the characteristics of the Hilbert–Huang transform, it can be well suited for research in the field of acoustic emission. In order to obtain more coal-rock instability mesostructure characteristics at different loading stages, Li Xuelong et al. used the HHT

method to analyze the acoustic emission waveform characteristics at different loading stages [21]. Kexin Liang et al. proposed a monitoring and early warning technology for internal cracks in the rail head. The data driving the algorithm can be obtained through Lamb wave finite element simulation and actual experiment of rail cutting. They used Shannon wavelet transform (SWT) to extract the first arrival wave and used Hilbert–Huang transform (HHT) to analyze its time-frequency characteristics [22]. In this paper, the signal is analyzed and processed using HHT after the experiment to obtain the IMF components in the main frequency range.

In this study, the non-contact SLDV technique is used to collect non-stationary A_0 wave signals in symmetry composite panel structures, and frequency characteristic parameters are obtained through HHT analysis of the vibration signals. The circular trajectory intersection method is employed to locate dynamic damage sources in panel structures with different material characteristics. The research aims to explore dynamic damage detection methods for composite panels in engineering structures.

2. The Basic Principle of Circular Trajectory Intersection Localization and Time-Domain CSM Imaging

The circular trajectory intersection method is a planar localization algorithm suitable for damage localization in plate structures [23]. It utilizes three or more sensors to collect signals on the plate structure and converts them into displacement or velocity signals. The relative time delays with respect to a reference sensor are then calculated and converted into distance differences. In this way, the time delays and distance differences obtained by multiple sensors form several circular trajectories. By comparing these circular trajectories, the region with the most concentrated intersection points can be identified to determine the location of the damage. The waves propagated in the thin plate structure employed in this paper are Lamb waves. The guided wave model in the frequency domain can be represented as $F(\omega)$,

$$F(\omega) = X(\omega) \left(\frac{1}{\sqrt{x}} \right) e^{-jk(\omega)x} \quad (1)$$

In Equation (1), $X(\omega)$ is a wave packet of Lamb waves, $1/\sqrt{x}$ represents the geometric loss in Lamb wave propagation, and, additionally, $j = \sqrt{-1}$ is the characteristic of dispersion. $k(\omega)$ represents the wave number in Lamb propagation. If the wave number is defined as $a\omega$, Equation (1) can be expressed using a non-dispersive equation:

$$M(\omega) = X(\omega) \left(\frac{1}{\sqrt{x}} \right) e^{-j\omega x} \quad (2)$$

where M signifies torque, $t = ax$, and the group velocity $C_g = 1/a$. In this experiment, the non-contact vibration modal signals acquired by SLDV laser are used, specifically the A_0 mode Lamb wave.

Figure 1 depicts a triangular sensor array consisting of sensors 1, 2, and 3, with r representing the distance between the ultrasonic source A and sensor 1. The angle between the line connecting the source and sensor 1 and the x -axis is denoted as θ . The distance difference between the source and sensors 1 and 2 is denoted as δ_1 , and the distance difference between the source and sensors 1 and 3 is denoted as δ_2 . The time differences between the arrival of the damage signal at sensors 1 and 2, and sensors 1 and 3, are represented as Δt_{12} and Δt_{13} , respectively. The propagation velocity of the ultrasonic wave is denoted as v . Based on the measured time differences, three circles can be drawn with the centers at the midpoint of sensors 1, 2, and 3, and radii of r , $r + \delta_1$, and $r + \delta_2$, respectively. The intersection points of the three circles represent the location of the ultrasonic source A.

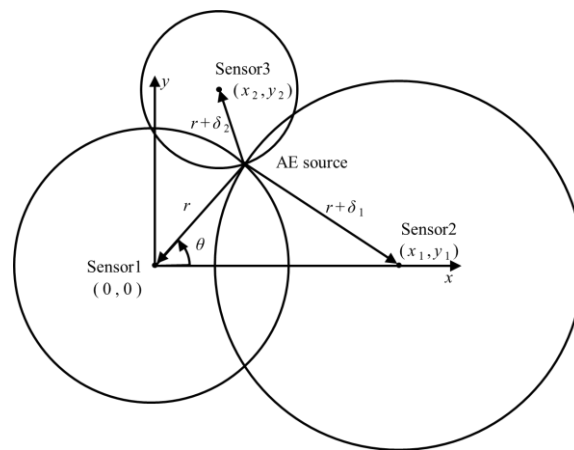


Figure 1. Schematic Diagram of Circular Trajectory Localization with Three Sensors.

Where the distance differences can be expressed as,

$$\delta_1 = v\Delta t_{12}, \quad \delta_2 = v\Delta t_{13} \quad (3)$$

Based on the geometric relationship,

$$r = \frac{A_1}{2(x_1 \cos \theta + y_1 \sin \theta + \delta_1)} = \frac{A_2}{2(x_2 \cos \theta + y_2 \sin \theta + \delta_2)} \quad (4)$$

where,

$$A_1 = x_1^2 + y_1^2 - \delta_1^2; \quad x_1 \cos \theta + y_1 \sin \theta + \delta_1 \neq 0 \quad (5)$$

$$A_2 = x_2^2 + y_2^2 - \delta_2^2; \quad x_2 \cos \theta + y_2 \sin \theta + \delta_2 \neq 0 \quad (6)$$

Simplifying Equation (4),

$$\theta = \arctan \frac{A_1 y_2 - A_2 y_1}{A_1 x_2 - A_2 x_1} \pm \arccos \left| \frac{A_2 \delta_1 - A_1 \delta_2}{B} \right| + 2m\pi \quad (7)$$

In Equation (7), $B = [(A_1 x_2 - A_2 x_1)^2 + (A_1 y_2 - A_2 y_1)^2]^{\frac{1}{2}}$, $m = 0, \pm 1, \pm 2$, where θ has two solutions within the range of $-\pi$ to π , but the value of θ must be chosen to make δ_2 positive. Based on Equations (4) and (7), the position of the ultrasonic source (x, y) can be determined as follows: $x = r \cos \theta$, $y = r \sin \theta$.

In general cases, there is only one ultrasound source; thus, a pair of time differences (Δt_{ba} and Δt_{ca}) is only valid when θ has a unique solution. When θ has two possible values, the position of the ultrasound source cannot be uniquely determined, resulting in one true and one false solution. To eliminate the false solution, a fourth ultrasound sensor can be added to obtain additional time difference data using the same hyperbolic localization principle. By analyzing the existing solutions, the position of the ultrasound source can be determined, and the false solution can be discarded. The Circular Trajectory Intersection Localization method provides an effective approach for determining the location of a target using multiple sensors. However, when dealing with non-linear and non-stationary ultrasonic wave signals, additional signal processing techniques are required to extract the relevant information accurately. The HHT method is a powerful tool for analyzing non-linear and non-stationary signals, making it a suitable candidate for enhancing the circular trajectory intersection localization method.

As shown in Figure 2, the plate-like structure is divided into grid cells of appropriate sizes. Figure 2a shows the signal receiving diagram of the SLDV rectangular array, and Figure 2b shows the signal receiving diagram of the ring DE-IDT array.

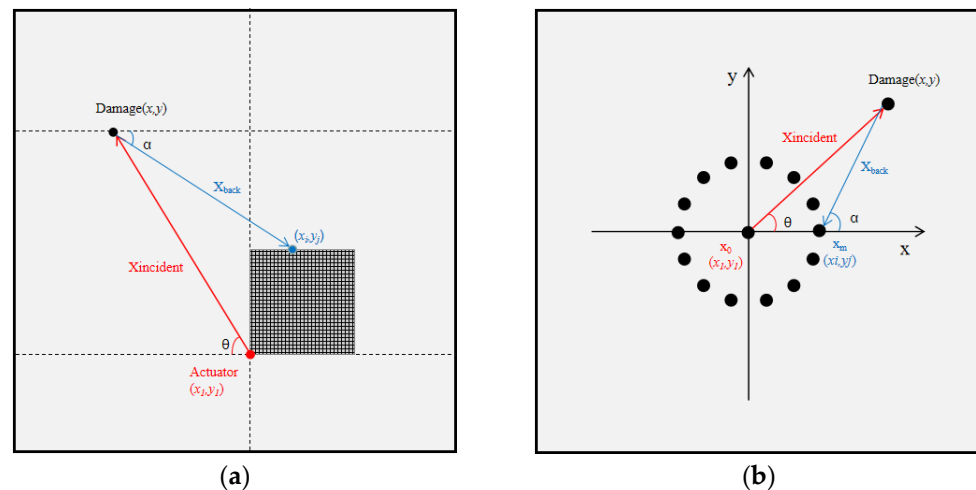


Figure 2. Time domain CSM imaging schematic. (a) The signal receiving diagram of SLDV rectangular array. (b) The signal receiving diagram of ring DE-IDT array.

Excitation source at coordinate (x_1, y_1) , receiving array element at coordinate (x_i, y_j) . Through the geometric relationship, the distance between the damage point and the excitation source and receiving point can be calculated, and its expression equation is shown as follows:

$$d_1(x, y) = \sqrt{(x - x_1)^2 + (y - y_1)^2} \tag{8}$$

$$d_{ij}(x, y) = \sqrt{(x - x_i)^2 + (y - y_j)^2} \tag{9}$$

Therefore, the transit time of the guided wave from the excitation source (x_1, y_1) to the damage point (x, y) can be expressed as:

$$t_1(x, y) = \frac{\sqrt{(x - x_1)^2 + (y - y_2)^2}}{c_{g,\theta}} \tag{10}$$

The transit time of the guided wave from the damage point (x, y) to the receiving point (x_i, y_j) can be expressed as:

$$t_2(x, y) = \frac{\sqrt{(x - x_i)^2 + (y - y_j)^2}}{c_{g,\alpha}} \tag{11}$$

where $c_{g,\theta}$ and $c_{g,\alpha}$ are the corresponding center frequency group velocities corresponding to different angles.

Since there is only one excitation source of CSM, the array signal is collected by the principle of one-dose and multiple-receive; thus, the total transit time of the guided wave from excitation source (x_1, y_1) to damage point (x, y) , and then from damage point (x, y) to receiving point (x_i, y_j) , can be expressed as:

$$t(x, y) = t_1(x, y) + t_2(x, y) = \frac{\sqrt{(x - x_1)^2 + (y - y_2)^2}}{c_{g,\theta}} + \frac{\sqrt{(x - x_i)^2 + (y - y_j)^2}}{c_{g,\alpha}} \tag{12}$$

By filling the signal amplitude of the corresponding time into the corresponding grid unit, the pixel of the corresponding grid unit on the board can be represented. Its expression equation is as follows:

$$A(x, y) = \sum_{i=1}^N \sum_{j=1}^M u_{ij}(t(x, y)) \tag{13}$$

In the equation are the number of elements in the x and y directions of the rectangular array, respectively, representing the time domain signals collected by different receiving array elements; the final $A(x, y)$ pixel matrix represents the imaging results.

3. Experimental Setup for Impact Source Localization on Composite Plate Based on SLDV

Due to the complex nature and anisotropic characteristics of composite symmetry plate structures, the propagation properties of stress waves are intricate. The non-contact laser detection method used to capture the A_0 mode signal of Lamb waves exhibits significant dispersion effects and nonlinearity. This leads to inaccurate propagation transit times, making it challenging to directly apply the circular trajectory intersection localization method for damage localization on the structure. Therefore, a waveform analysis method based on HHT is employed. In this approach, the obtained raw damage signals are subjected to Intrinsic Mode Function (IMF) decomposition through HHT. This allows for the effective identification of the signals containing relevant damage features and discrimination from noise. Information related to material damage is extracted, and a corresponding database of damage features is established.

The experimental setup uses a PSV-500 SLDV vibrometer. Figure 3 shows the non-contact signal acquisition setup for impact source in fiberglass composite plates. The setup is used to test a $1000 \times 1230 \text{ mm} \times 10 \text{ mm}$ single-layer composite plate made of 45° glass fiberglass board-reinforced epoxy resin. The surface of the plate is marked with 8 signal acquisition points (1–8) where retroreflective stickers are placed, and there are 4 impact points for simulating impact signals. The plate is struck at points A, B, C, D using a small iron hammer, and the signals are collected using the SLDV. If the knocking energy is too large, the waveform distortion will be caused; thus, it is necessary to repeat the knocking several times, so that the repeatability of the waveform is good.

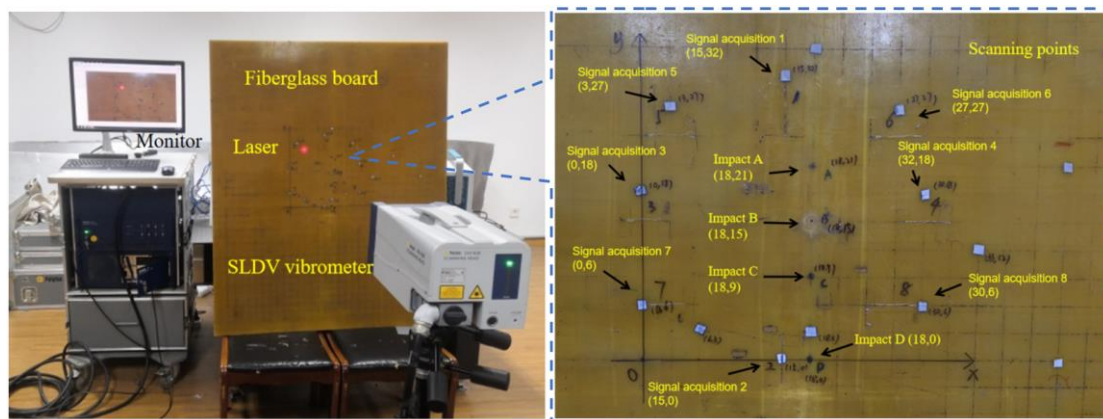


Figure 3. Experimental setup for non-contact acquisition of impact source in fiberglass composite plates.

4. Impact Source Localization Results

In the experiment, SLDV is used to non-contactly collect experimental data of the out-of-plane vibration modal signals from four groups of plate structures. Among them, one group of experimental data, denoted as a1~a4, is selected and imported into the HHT impact source algorithm for processing and analysis. The number of data points collected is $2^{14} = 16,384$, and the sampling frequency is 5.12 MHz. The steps of the vibration measurement experiment are as follows: (1) Start the system. (2) Acquire the shape data using the laser probe. (3) Define the grid. (4) Focus the laser point. (5) Start scanning and save the received signals. The collected data are represented by a time axis on the horizontal axis and a velocity parameter on the vertical axis.

The ultrasonic signal data from each group is decomposed using Empirical Mode Decomposition (EMD) to obtain the Hilbert spectrum. The extracted IMFs exhibit a gradual

decrease in frequency. EMD decomposition arranges the components in order of decreasing frequency, with the highest frequency component, IMF1, being extracted first, followed by gradually decreasing frequencies. By comparing waveform information and considering the characteristics of the impact signal, the corresponding IMF components that constitute the effective components of the signal can be determined.

In this experiment, Figure 4 shows that the waveforms of the first three IMFs are relatively weak, while the waveforms of IMF4, IMF5, IMF6, and IMF7 contain complete and significant information. The amplitude of the impact characteristic signal is large. By performing Hilbert transform on the IMFs and reconstructing the time-domain signal, unrequired frequency components are removed while preserving the essential components. By extracting the IMF with the maximum amplitude and performing Hilbert transform reconstruction, the 3D Hilbert spectrum shown in Figure 5a–d is obtained. Most of the energy is concentrated in the low-frequency range, which corresponds to the low-frequency characteristics of impact vibration signals. By observing the amplitude dimension, it is typically found that the first peak represents the damage signal.

The experiment involves using SLDV technology to obtain the out-of-plane vibration signals of the composite material plate caused by impacts and measure their displacement information. The signals are then analyzed and processed using HHT to obtain IMF components in four major frequency ranges. By removing unnecessary frequency components and retaining the relevant information, signal filtering is achieved. After selecting the characteristic IMF, the Hilbert spectrum is obtained through Hilbert transformation. In waveform analysis, HHT possesses adaptive characteristics, allowing for the generation of time-frequency energy spectra and extraction of IMF. This method can effectively reflect various sound source mechanisms and the extent of component damage, making it versatile in its application.

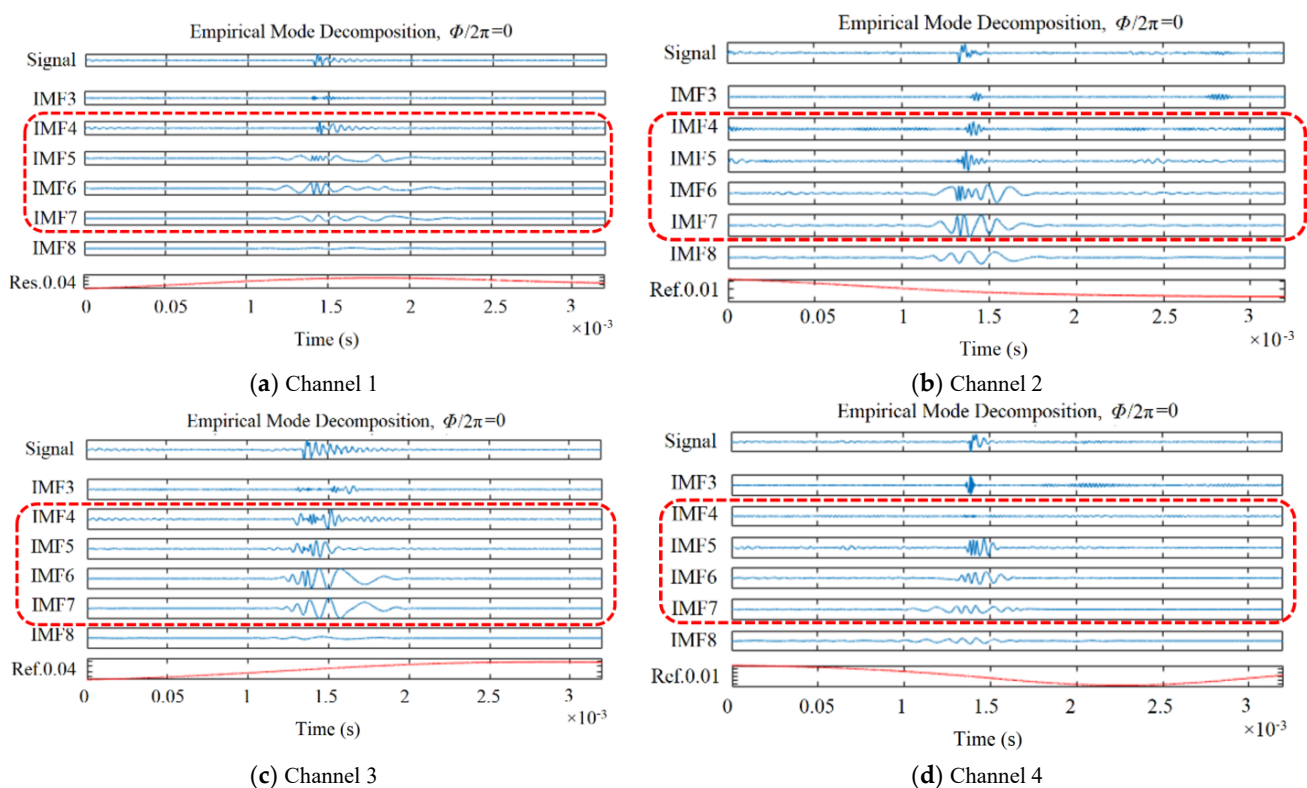


Figure 4. IMF of each order obtained by EMD decomposition: (a–d), respectively, correspond to the EMD decomposition diagrams of the signals at points 1 to 4.

To eliminate the influence of multiple reflections and improve the accuracy of target damage localization, an experimental setup is used, as shown in Figure 3. Eight-channel

signals are obtained for circular trajectory intersection imaging. The spacing between each signal receiving point is 25 mm. Based on HHT analysis of the signals received by SLDV, EMD decomposition is performed to obtain a series of Intrinsic Mode Functions (IMFs) representing different time-scale characteristics. The Hilbert spectrum features of the IMFs are also obtained. The time-domain waveform of IMF4, which is associated with the impact frequency, is extracted. Using Equations (2) and (3), different amplitude distributions corresponding to the reflection time are allocated to possible circular trajectory points. Figure 6a,b show the circular trajectory localization imaging results for points A and D with impact-induced source, respectively. The black circles represent the actual damage locations at A (180, 210) and D (180, 0), while the darker red positions indicate the localized damage center positions. The center localization errors are 7 mm and 5 mm, respectively. The experimental results demonstrate that the damage detection accuracy is significantly improved by using the circular trajectory localization method after HHT analysis.

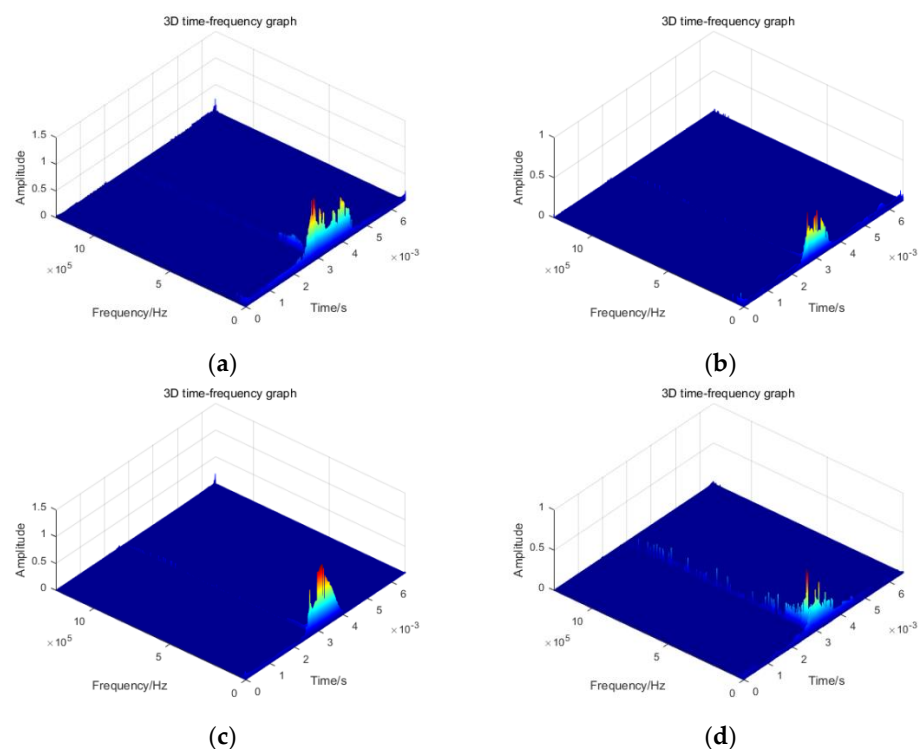


Figure 5. Hilbert Spectrum: (a–d) correspond to the 3D Hilbert spectra of signals from points 1 to 4.

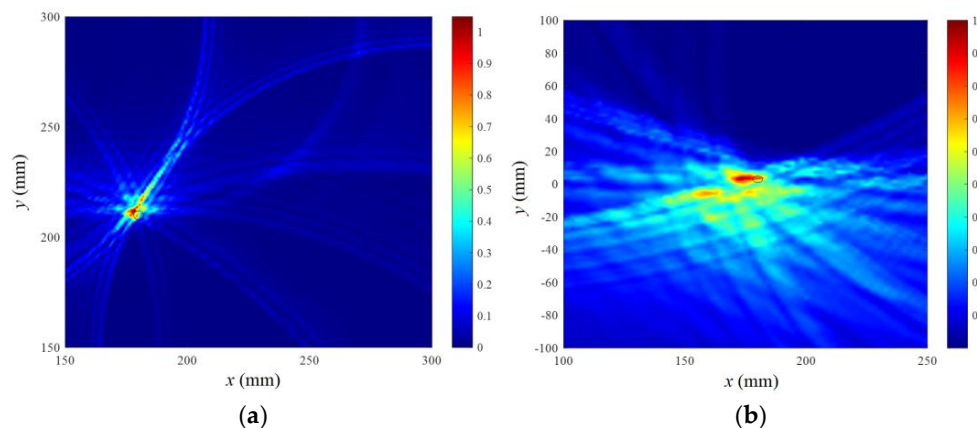


Figure 6. Damage imaging results using circular trajectory localization on fiberglass board: (a) Image of impact localization at point A; (b) image of impact localization at point B.

5. Conclusions

In order to identify the dynamic damage in engineering structures accurately and to verify the effectiveness of random impact on contact-based sensor detection for impact localization, this study is based on the weak S_0 modal signal generated by ultrasonic Lamb waves in the low-frequency range. It utilizes non-contact SLDV to collect the non-stationary A_0 wave signal in the composite material board structure and applies HHT analysis to extract frequency feature parameters from the vibration signal and perform filtering and noise reduction. Finally, the circular trajectory intersection method is employed to achieve precise localization of dynamic damage sources in plate structures with different material properties. This provides a method for the dynamic damage detection of composite symmetry material boards in practical engineering structures. Compared with the Lamb wave detection results [1,2], the algorithm shows it is imaging faster and fit for the composite material.

Author Contributions: Conceptualization, Z.W.; methodology, Z.W. and J.Z.; validation, Z.W. and J.Z.; investigation, H.C. and R.G.; writing—original draft preparation, Z.W. and J.Z.; writing—review and editing, R.G. and Y.Z. All authors have read and agreed to the published version of the manuscript.

Funding: This research was funded by China Scholarship Council (No.202008320084), the National Natural Science Foundation of China (No.11872191), Foreign Expert Project of Chinese Ministry of Science Technology (DL2022014011L) and Postgraduate Research & Practice Innovation Program of Jiangsu Province (KYCX23_3741 and KYCX22_3615).

Data Availability Statement: The authors of this study were unable to find a valid data repository for the data produced in this study. But we can share the data as request from the author.

Acknowledgments: Thanks all the authors for their contribution to the research work and thanks to Yang Zhang for contacting European Cooperation in Science and Technology CA21155, CA18203 and providing relevant open source knowledge.

Conflicts of Interest: The authors declare no conflict of interest regarding the publication of this paper.

References

1. Alshits, V.I.; Lothe, J. Some basic properties of bulk elastic waves in anisotropic media. *Wave Motion* **2004**, *40*, 297–313. [[CrossRef](#)]
2. Fernando, Z.; Kirill, V.L. Wave-based optical coherence elastography: The 10-year perspective. *Prog. Biomed. Eng.* **2022**, *4*, 012007.
3. Sang, S.; Sandgren, E. Study of in-plane wave propagation in 2-dimensional anisotropic elastic metamaterials. *J. Vib. Eng. Technol.* **2019**, *7*, 63–72. [[CrossRef](#)]
4. Tao, C.; Zhang, C.; Ji, H.; Qiu, J. Fatigue damage characterization for composite laminates using deep learning and laser ultrasonic. *Compos. Part B Eng.* **2021**, *216*, 108816. [[CrossRef](#)]
5. Purekar, A.S.; Pines, D.J. Damage Detection in Thin Composite Laminates Using Piezoelectric Phased Sensor Arrays and Guided Lamb Wave Interrogation. *J. Intell. Mater. Syst. Struct.* **2010**, *21*, 995–1010. [[CrossRef](#)]
6. Chang, J.; Zheng, C.; Ni, Q.Q. The ultrasonic wave propagation in composite material and its characteristic evaluation. *Compos. Struct.* **2006**, *75*, 451–456. [[CrossRef](#)]
7. Wang, L.; Yuan, F.G. Lamb wave propagation in composite laminates using a higher-order plate theory. In Proceedings of the SPIE—The International Society for Optical Engineering, San Diego, CA, USA, 18–22 March 2007.
8. Pant, S.; Laliberte, J.; Martinez, M.; Rocha, B.; Ancrum, D. Effects of composite lamina properties on fundamental Lamb wave mode dispersion characteristics. *Compos. Struct.* **2015**, *124*, 236–252. [[CrossRef](#)]
9. Hu, Z.; An, Z.; Kong, Y.; Lian, G.; Wang, X. The nonlinear S_0 Lamb mode in a plate with a linearly-varying thickness. *Ultrasonics* **2018**, *94*, 102–108. [[CrossRef](#)]
10. Jun, Y.J.; Park, I.W.; Lee, U.S. A Method of Lamb-Wave Modes Decomposition for Structural Health Monitoring. *J. Korean Soc. Precis. Eng.* **2012**, *29*, 887–895. [[CrossRef](#)]
11. Raghavan, A.C.; Cesnik, C.E.S. Review of Guided-Wave Structural Health Monitoring. *Shock Vib. Dig.* **2007**, *39*, 91–114. [[CrossRef](#)]
12. Ahmadi, H.R.; Mahdavi, N.; Bayat, M. A novel damage identification method based on short time Fourier transform and a new efficient index. *Structures* **2021**, *33*, 3605–3614. [[CrossRef](#)]
13. Daubechies, I. The wavelet transform, time-frequency localization and signal analysis. *IEEE Trans. Inf. Theory* **1990**, *36*, 961–1005. [[CrossRef](#)]
14. Chang, H.Y.; Yuan, F.G. Visualization of hidden damage from scattered wavefield reconstructed using an integrated high-speed camera system. *Struct. Health Monit.* **2021**, *20*, 2300–2316. [[CrossRef](#)]

15. Wang, Z.; Fei, Y.; Li, B.; Zhou, A.; Gorgin, R. Research on the f-k Domain Multimodal Damage Detection Imaging Fusion Method in Metal Plate. *Trans. Indian Inst. Met.* **2022**, *75*, 2777–2786. [[CrossRef](#)]
16. Stankovic, L.; Alieva, T.; Bastiaans, M.J. Time-frequency signal analysis based on the windowed fractional Fourier transform. *Signal Process.* **2003**, *83*, 2459–2468. [[CrossRef](#)]
17. Wu, J.; Xu, X.; Liu, C.; Deng, C.; Shao, X. Lamb wave-based damage detection of composite structures using deep convolutional neural network and continuous wavelet transform. *Compos. Struct.* **2021**, *276*, 114590. [[CrossRef](#)]
18. Sang, S.; Sandgren, E.; Wang, Z. Wave attenuation and negative refraction of elastic waves in a single-phase elastic metamaterial. *Acta Mech.* **2018**, *229*, 2561–2569. [[CrossRef](#)]
19. Huang, N.E.; Long, S.R.; Shen, Z. The mechanism for frequency downshift in nonlinear wave evolution. *Adv. Appl. Mech.* **1996**, *32*, 59–117C.
20. Souza, U.B.; Escola, J.P.L.; da Cunha Brito, L. A survey on Hilbert-Huang transform: Evolution, challenges and solutions. *Digit. Signal Process.* **2022**, *120*, 103292. [[CrossRef](#)]
21. Li, X.; Chen, S.; Liu, S.; Li, Z.H. AE waveform characteristics of rock mass under uniaxial loading based on Hilbert-Huang transform. *J. Cent. South Univ.* **2021**, *28*, 1843–1856. [[CrossRef](#)]
22. Liang, K.; Zhang, Y.; Cai, G. Monitoring and Early Warning Technology for Internal Cracks of Railhead Based on Lamb Wave. In Proceedings of the Recent Developments in Mechatronics and Intelligent Robotics: Proceedings of ICMIR 2019 3, Kunming, China, 25–26 May 2019.
23. Espinosa Peralta, P.; Luna, M.A.; de la Puente, P.; Campoy, P.; Bavle, H.; Carrio, A.; Cruz Ulloa, C. Performance Analysis of Localization Algorithms for Inspections in 2D and 3D Unstructured Environments Using 3D Laser Sensors and UAVs. *Sensors* **2022**, *22*, 5122. [[CrossRef](#)]

Disclaimer/Publisher's Note: The statements, opinions and data contained in all publications are solely those of the individual author(s) and contributor(s) and not of MDPI and/or the editor(s). MDPI and/or the editor(s) disclaim responsibility for any injury to people or property resulting from any ideas, methods, instructions or products referred to in the content.